

# Tunable directive radiation of surface-plasmon diffraction gratings

Youngkyu Lee,<sup>1</sup> Kazunori Hoshino,<sup>2</sup> Andrea Alù,<sup>1</sup>  
and Xiaojing Zhang<sup>2,\*</sup>

<sup>1</sup>Department of Electrical and Computer Engineering, 1 University Station, TX, Austin, 78712, USA

<sup>2</sup>Department of Biomedical Engineering, 1 University Station, TX, Austin, 78712, USA

\*John.Zhang@enr.utexas.edu

**Abstract:** We experimentally demonstrate tunable radiation from a periodic array of plasmonic nanoscatterers, tailored to convert surface plasmon polaritons into directive leaky modes. Extending our previous studies on efficient directional beaming based on leaky-wave radiation from periodic gratings driven by a subwavelength slit, we experimentally show dynamic beam sweeping by tuning the directional leaky-wave mechanism in real-time. Two alternative tuning mechanisms, wavelength- and index-mediated beam sweeping, are employed to modify the relative phase of scattered light at each grating edge and provide the required modification of the radiation angle.

©2013 Optical Society of America

OCIS codes: (050.1220) Apertures; (240.6680) Surface plasmons.

---

## References and links

1. J. Li, A. Salandrino, and N. Engheta, "Shaping light beams in nanometer scale: A Yagi-Uda nanoantenna in the optical domain," *Phys. Rev. B* **76**(24), 245403 (2007).
2. T. Kosako, Y. Kadoya, and H. F. Hofmann, "Directional control of light by a nano-optical Yagi-Uda antenna," *Nat. Photonics* **4**(5), 312–315 (2010).
3. A. G. Curto, G. Volpe, T. H. Taminiau, M. P. Kreuzer, R. Quidant, and N. F. van Hulst, "Unidirectional emission of a quantum dot coupled to a nanoantenna," *Science* **329**(5994), 930–933 (2010).
4. H. F. Hofmann, T. Kosako, and Y. Kadoya, "Design parameters for a nano-optical Yagi-Uda antenna," *New J. Phys.* **9**(7), 217 (2007).
5. T. H. Taminiau, F. D. Stefani, and N. F. van Hulst, "Enhanced directional excitation and emission of single emitters by a nano-optical Yagi-Uda antenna," *Opt. Express* **16**(14), 10858–6 (2008).
6. G. Pellegrini, G. Mattei, and P. Mazzoldi, "Tunable, directional and wavelength selective plasmonic nanoantenna arrays," *Nanotechnology* **20**(6), 065201 (2009).
7. A. F. Koenderink, "Plasmon nanoparticle array waveguides for single photon and single plasmon sources," *Nano Lett.* **9**(12), 4228–4233 (2009).
8. T. Coenen, E. J. R. Vesseur, A. Polman, and A. F. Koenderink, "Directional emission from plasmonic Yagi-Uda antennas probed by angle-resolved cathodoluminescence spectroscopy," *Nano Lett.* **11**(9), 3779–3784 (2011).
9. X. X. Liu and A. Alù, "Subwavelength leaky-wave optical nanoantennas: Directive radiation from linear array of plasmonic nanoparticles," *Phys. Rev. B* **82**(14), 144305 (2010).
10. T. W. Ebbesen, H. J. Lezec, H. F. Ghaemi, T. Thio, and P. A. Wolff, "Extraordinary optical transmission through sub-wavelength hole arrays," *Nature* **391**(6668), 667–669 (1998).
11. H. J. Lezec, A. Degiron, E. Devaux, R. A. Linke, L. Martin-Moreno, F. J. Garcia-Vidal, and T. W. Ebbesen, "Beaming light from a subwavelength aperture," *Science* **297**(5582), 820–822 (2002).
12. S. Kim, H. Kim, Y. Lim, and B. Lee, "Off-axis directional beaming of optical field diffracted by a single subwavelength metal slit with asymmetric dielectric surface gratings," *Appl. Phys. Lett.* **90**(5), 051113 (2007).
13. H. Kim, J. Park, and B. Lee, "Tunable directional beaming from subwavelength metal slits with metal-dielectric composite surface gratings," *Opt. Lett.* **34**(17), 2569–2571 (2009).
14. F. Hao, R. Wang, and J. Wang, "A design methodology for directional beaming control by metal slit-grooves structure," *J. Opt.* **13**(1), 015002 (2011).
15. S. Kim, Y. Lim, H. Kim, J. Park, and B. Lee, "Optical beam focusing by a single subwavelength metal slit surrounded by chirped dielectric surface gratings," *Appl. Phys. Lett.* **92**(1), 013103 (2008).
16. P. Chen, Q. Gan, F. J. Bartoli, and L. Zhu, "Near-field-resonance-enhanced plasmonic light beaming," *IIEEE Photon. J.* **2**(1), 8–17 (2010).
17. H. Kim and B. Lee, "Unidirectional surface plasmon polariton excitation on single slit with oblique backside illumination," *Plasmonics* **4**(2), 153–159 (2009).
18. Y. Lee, K. Hoshino, A. Alù, and X. J. Zhang, "Efficient directional beaming from small apertures using surface-plasmon diffraction gratings," *Appl. Phys. Lett.* **101**(4), 041102 (2012).

19. Y. Lee, A. Alù, and J. X. Zhang, "Efficient apertureless scanning probes using patterned plasmonic surfaces," *Opt. Express* **19**(27), 25990–25999 (2011).
20. A. A. Oliner and D. R. Jackson, *Antenna Engineering Handbook*, 4th ed. (McGraw-Hill, New York, 2007).
21. C. A. Balanis, *Antenna Theory Analysis and Design*, 3rd ed. (John Wiley & Sons, 2005).
22. F. López-Tejiera, S. G. Rodrigo, L. Martín-Moreno, F. J. García-Vidal, E. Devaux, T. W. Ebbesen, J. R. Krenn, I. P. Radko, S. I. Bozhevolnyi, M. U. González, J. C. Weeber, and A. Dereux, "Efficient unidirectional nanoslit couplers for surface plasmons," *Nat. Phys.* **3**(5), 324–328 (2007).
23. L. VJ, N. P. Kobayashi, M. S. Islam, W. Wu, P. Chaturvedi, N. X. Fang, S. Y. Wang, and R. S. Williams, "Ultrasoft silver film deposited with a germanium nucleation layer," *Nano Lett.* **9**, 178–182 (2009).
24. J. Y. Laluet, A. Drezet, C. Genet, and T. W. Ebbesen, "Generation of surface plasmons at single subwavelength slits: from slit to ridge plasmon," *New J. Phys.* **10**(10), 105014 (2008).
25. P. Lalanne, J. P. Hugonin, and J. C. Rodier, "Theory of Surface Plasmon Generation at Nanoslit Apertures," *Phys. Rev. Lett.* **95**(26), 263902 (2005).
26. P. Lalanne and J. P. Hugonin, "Interaction between optical nano-objects at metallo-dielectric interfaces," *Nat. Phys.* **2**(8), 551–556 (2006).
27. Q. Gan, Y. Gao, Q. Wang, L. Zhu, and F. Bartoli, "Surface plasmon waves generated by nanogrooves through spectral interference," *Phys. Rev. B* **81**(8), 085443 (2010).
28. E. Kretschmann and H. Raether, "Radiative decay of non-radiative surface plasmons excited by light," *Z. Naturforsch. A* **23**, 2135–2136 (1968).

## 1. Introduction

Tailoring the electromagnetic radiation of an array of antennas is a classic subject of interest in many research areas since its first explorations in 1905 by Karl Ferdinand Braun. At microwaves and radio frequencies, phased arrays are commonly used to scan a directive radiation pattern in the angular spectrum. By manipulating the relative phase of the signal feeding each antenna element, radiation can be pointed towards the desired direction and suppressed in all others. One useful feature provided by phased arrays is dynamic beam sweeping: by actively modifying the phase with which each element is driven, it is possible to tailor the overall radiation towards an arbitrary direction and suppress undesired radiation in other directions. A similar approach may be applied in plasmonic nano-optics, where an array of small scatterers [1–9] may be used to realize directive optical radiation. By modifying the phase of the excitation of each radiator, the collective optical radiation may be directed and dynamically manipulated towards the direction of interest. Recently, Yagi-Uda nanoantennas [1–5,8] consisting of parasitically phased elements driven by a confined quantum source have been demonstrated at optical frequencies, providing directional emission from the nanoscale to the far-field. Similarly, slit-based patterned planar surfaces have been reported showing directive optical radiation [10–17]. Albeit various design efforts have been spent to develop directive and controlled radiation for relevant applications in nano-optics, limited experimental efforts showing the possibility of dynamic beam sweeping have been reported [11].

In this paper, we focus on a nanopatterned metallic surface over which tunable directional optical radiation is realized using a subwavelength slit coupled on one side to an array of periodic gratings. The directive radiation is based on the leaky-wave mode supported by the periodic structure in a given frequency band of interest. In the proposed configuration, the subwavelength slit excites the array over a plasmonic screen, launching surface plasmon polaritons (SPPs) that are converted into leaky modes by the proper periodic corrugations. The coupling between the excitation and the SPP mode is maximized by controlling the slit width through nanofabrication and the angle of excitation, so that SPPs are generated primarily on the grating side [17–19] to maximize the coupling efficiency with the leaky-wave mode [18]. This solution has also the advantage of suppressing the conventional slit diffraction and unwanted side lobes for a specifically optimized oblique angle of illumination. Similar to radio-frequency leaky-wave antennas [20,21], it is then possible to sweep the direction of optical radiation by manipulating the effective electrical distance between the scatterers.

## 2. Design of tunable optical phased array

The proposed optical phased array consists of an array of periodic metal bumps driven by a slit aperture, which couples incident transverse-magnetic (TM) light into plasmonic modes. In this configuration, shown in Fig. 1, a one-dimensional (1D) array of periodic metal bumps serves as a directive optical antenna, effectively converting the dominant SPP mode into a leaky-wave mode radiating in free space. Previously we have studied efficient directive radiation from metal bumps excited by SPPs [18].

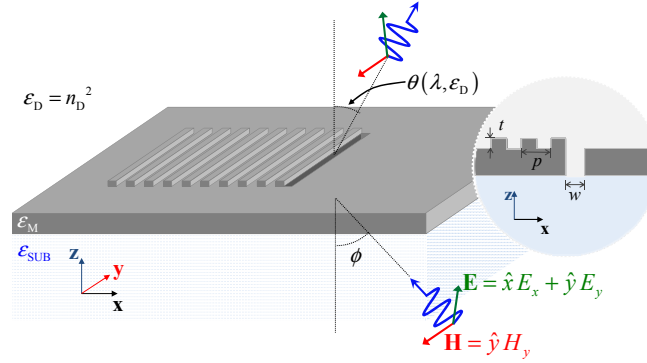


Fig. 1. Schematic of a tunable directional optical antenna: a subwavelength slit with a left-side array of periodic gratings, consisting of corrugations in a plasmonic screen. Note that  $\epsilon_D$ ,  $\epsilon_M$ , and  $\epsilon_{SUB}$  indicate the relative permittivity of surrounding medium, metal, and supporting substrate (BK7), respectively. Directive radiation at a specific angle  $\theta$  can be achieved by a proper choice of surrounding medium  $\epsilon_D$  and wavelength  $\lambda$  of operation; and its directivity can be further enhanced by optimizing illumination angle  $\phi$ .

In our model, we have shown that the phase matching condition to form a collimated directive leaky-mode within the first diffraction order of each scatterer is given by

$$p(\text{Re}[k_{SP}] + k_D \sin \theta) = 2\pi, \quad (1)$$

where, the SPP wavenumber is  $k_{SP} = 2\pi[(\epsilon_M \epsilon_D)/(\epsilon_M + \epsilon_D)]^{1/2}/\lambda$ , which is perturbed into a directive leaky-wave mode with wavenumber  $k_D = 2\pi\sqrt{\epsilon_D}/\lambda$  by the periodic corrugations,  $\epsilon_D$  is the dielectric permittivity of background,  $\epsilon_M$  is the metal permittivity,  $\theta$  is the angle of radiation, and  $p$  is the array periodicity. We assume that the permittivity of all involved materials is dispersive hence a function of the operating wavelength  $\lambda$ . Since the effective electrical length  $p \cdot \text{Re}[k_{SP}]$  and  $p \cdot k_D \sin \theta$ , governing the matching condition Eq. (1), are controllable by the operating wavelength and background permittivity, we may tune the direction of optical radiation by tuning either one of these quantities. Following the design methodology [18], we choose initial design parameters to realize maximum radiation at  $\theta = 25^\circ$  for operating wavelength  $\lambda = 630$  nm and free space ( $\epsilon_D = 1$ ). It is important to note that the proposed configuration can tailor light into any propagating mode of interest. Even though we focus on coupling energy to free-space with leaky modes, light may also be coupled to surface plasmon modes by properly choosing the design parameters [22].

For the excitation of such optical phased array consisting of periodic metal bumps, a perforated slit in plasmonic screen is chosen to serve as a driving element, providing efficient conversion of incident TM light into surface plasmon modes [17–19]. With tilted illumination, a perforated slit that supports higher-order guided modes can provide

unidirectional generation of SPP at its exit, maximizing the radiation efficiency of this system. The mode supported by a plasmonic slit follows the dispersion equation

$$i \left[ w(-\beta^2 + k_D^2)^{1/2} - m\pi \right] = 2 \tan h^{-1} \left[ i\epsilon_D (\beta^2 - \epsilon_M k_D^2)^{1/2} / \epsilon_M (-\beta^2 + k_D^2)^{1/2} \right]. \quad (2)$$

A slit width  $w = 300$  nm is therefore chosen to support the higher-order ( $m = 1$ ) guided mode, which may couple energy into the desired SPP only on the side of the grating for a specific excitation angle.

### 3. Device fabrication and experimental characterization

We adopted nanofabrication technologies capable of producing sub-100 nm feature size to realize such optical phased array as in Fig. 1. First, 250 nm thick Ag film was deposited on BK7 slide with 3 nm thick Ge layer serving as a wetting layer [23] to enhance adhesion and surface quality of the Ag film. Opposite to the case presented in Ref 24, the thickness of the Ag film was chosen to be thick enough so that SPPs at the metal/BK7 interface would not leak through the film for the case the of surrounding index  $n_D$  is higher than that of BK7. An array of Ag bumps on the surface, with periodicity  $p = 414$  nm and duty ratio 0.5, was formed on the Ag film to provide a 1st order plasmonic grating diffraction. General E-beam lithography (JEOL 6000 FSE, JEOL Ltd, Tokyo, Japan) and lift-off techniques were used with a bi-layer PMMA process (495K C4/950K C4, MicroChem Inc., MA, USA) to construct a  $t = 60$  nm height array of gratings. A slit was then defined and perforated in Ag film right next to the array by focused ion beam (FEI SEM/FIB dual beam, FEI Corp., OR, USA) milling. The milled slit had a width of 300 nm to support a higher-order mode of slit transmission, necessary for high coupling efficiency [17–19] and improved directive radiation [18], as discussed in the previous section. The distance between the left-most slit edge and the first rising edge of the corrugations was kept to 0 nm, following our theoretical investigations [18]. Finally, on top of the fabricated plasmonic configuration (consistent with Fig. 1), flat BK7 coverslip ( $\sim 200$   $\mu\text{m}$  in thickness) was added with 80  $\mu\text{m}$  thick PDMS spacer to create a space to introduce various index matching fluids (Cargille-Sacher Laboratories Inc., NJ, USA).

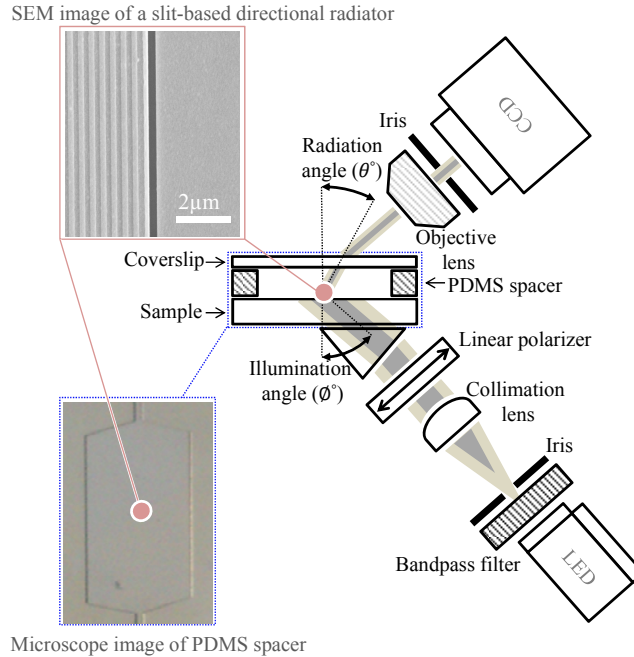


Fig. 2. Schematic of the optical setup to measure far-field radiation patterns. Embedded pictures: a scanning electron micrograph (SEM) of the fabricated device (top) and microscope image of PDMS spacer (bottom).

The radiation patterns from the fabricated device were then characterized with a custom optical setup allowing us to control the angle of both illumination and radiation. The angular intensity profile was recorded on a CCD, as shown in Fig. 2. A 300 nm slit was excited with oblique backside illumination of a collimated TM plane-wave at a specific wavelength of operation. A broadband white light emitting diode (LED) was used with a bandpass filter to acquire the desired spectra at the output. Angular-dependent optical signals from the device were collected with low numerical aperture (NA) optics (Olympus LMPlan X20/0.4 with closed iris) and captured by a charge-coupled device (CCD). The fabricated device and illumination optics were mounted on separate three-axis alignment systems with rotational stage, allowing for the control of both illumination and measurement angles. Detailed intensity profiling for angular dependent radiation are provided in Fig. 3.

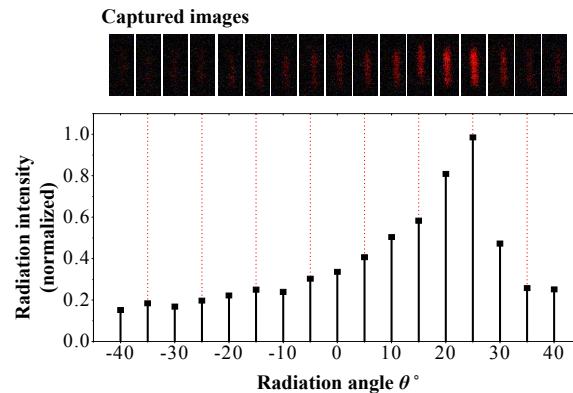


Fig. 3. Radiation pattern profiles from CCD images captured at various angles for  $\lambda = 630$  nm and no index matching fluid in the spacer.

#### 4. Experimental results and discussion

We experimentally demonstrate a tuning mechanism for directional radiation and beam sweeping in this setup (see Fig. 1 and Fig. 2), obtained by changing the background medium around the corrugations. As typical in leaky-wave antenna setups [20,21], we are also able to track the single-beam sweeping associated with varying the wavelength of operation. Along with the characterization of tunable directive radiation, we also discuss and verify that efficient SPP coupling can be an effective tool to improve the directionality under index-mediated tuning mechanisms. Our experimental setup does not allow to directly evaluate the SPP coupling efficiency [25–27] through a slit to extract the overall radiation efficiency of the proposed configuration, but we use modal spectral analysis for this purpose. By measuring the full-width-at-half-maximum (FWHM) angle of radiation, the proposed configuration can be qualitatively characterized. Since the diffraction grating supports directive radiation at a specific angle, efficient generation of SPPs toward gratings and conversion into directive leaky mode will result in sharper angular response [18]. Measured radiation patterns for the two tuning mechanisms are presented in Fig. 4.

In Fig. 4(a), radiation patterns were recorded after varying the index range of matching fluids  $n_D = \epsilon_D^{1/2} = 1.26 \sim 1.62$  at the fixed wavelength  $\lambda = 630$  nm. We note that the weak frequency dispersion of each index matching fluid is not significant within the spectral bandwidth considered in each measurement, as it is contained within an index variation of less than 0.001. In illuminating the slit, we used TM polarized light at the operating wavelength with 10 nm of spectral FWHM bandwidth. In Fig. 4(b), conversely, we show beam scanning changing the wavelength of illumination ( $\lambda = 500 \sim 650$  nm), in the absence of index matching fluids ( $n_D = 1$ ). Also here, the spectral FWHM for each illumination was 10 nm. To compare the angular shift and the angular confinement of radiation pattern (angular FWHM) for both tuning mechanisms, each recorded pattern in Fig. 4 is normalized with respect to its peak radiation intensity.

As seen in Fig. 4, we have experimentally demonstrated the two tuning mechanisms scanning directive radiation. By varying the background refractive index ( $n_D = 1.00 \sim 1.62$ ), we achieve a shift of peak radiation angle of about  $39.7^\circ$ ; and by varying the wavelength of operation  $\lambda$  from 500 nm to 650 nm, the peak radiation angle  $\theta$  changes from  $-1^\circ$  to  $+27^\circ$ . Detailed angular sensitivity of directive radiation with respect to these tuning mechanisms is summarized in Fig. 5. As expected, nearly linear variation with the angle of radiation is found, both in terms of wavelength of operation and of change in the refractive index. The angle may scan from positive values to broadside radiation, with interesting implications for beam scanning, optical communications and plasmonic sensors at the molecular scale.

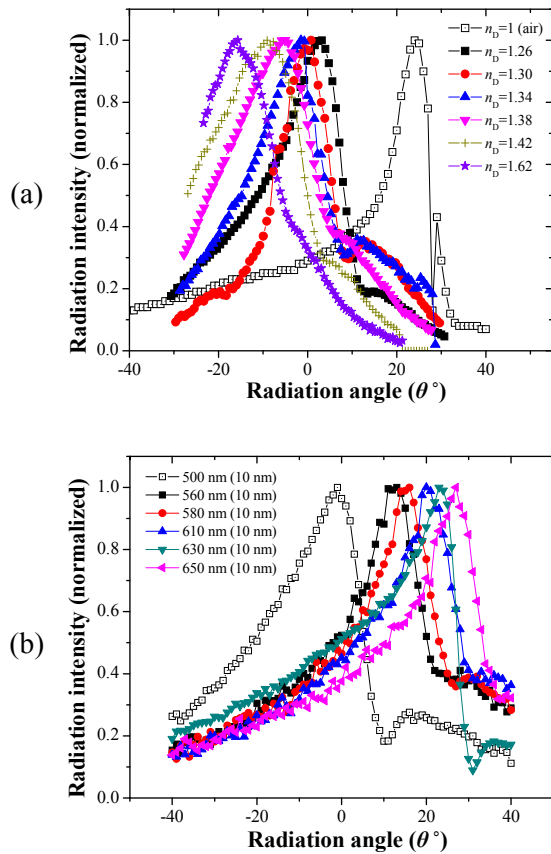


Fig. 4. Measured far-field radiation patterns from the proposed configuration with (a) various index matching fluids and (b) various wavelengths of operation. TM polarized light with spectral FWHM of 10 nm was used throughout experiments. Note that each recorded radiation pattern is normalized to its peak intensity.

Throughout the experiments, the illumination angle  $\phi$  was carefully selected at each wavelength and each index matching fluid to maximize the coupling efficiency with the SPP toward the grating side, according to the theory presented in [17–19]. Since the modal propagation inside the slit is a function of both wavelength and the refractive index of the fluid, as well as the geometric parameters, different values of illumination angles had to be selected in each experiment. The evidence of improved directive optical radiation with an idea of tilted illumination of slit can be found in Fig. 6 for one of the experimental results, for an index matching fluid  $n_D = 1.34$  and wavelength  $\lambda = 630$  nm. By exciting the slit at normal incidence and at the optimized incidence angle of  $26^\circ$ , we find a drastic difference in overall radiation directivity, achieved by suppressing the unwanted side lobe and reducing the angular FWHM of the radiation pattern from  $36.0^\circ$  to  $19.1^\circ$ . As expected, the radiation peak is mostly the same for the two excitations, since the leaky-mode supported by the grating is not affected by the SPP excitation mechanism. These results are consistent with our previous studies on efficient directional beaming [18]. Similar to the case of SPPs guided toward diffraction gratings, herein the overall directivity can be drastically improved by optimizing the slit width and the angle of illumination to properly couple SPPs to the grating and eliminate undesired diffraction effects from the slit.

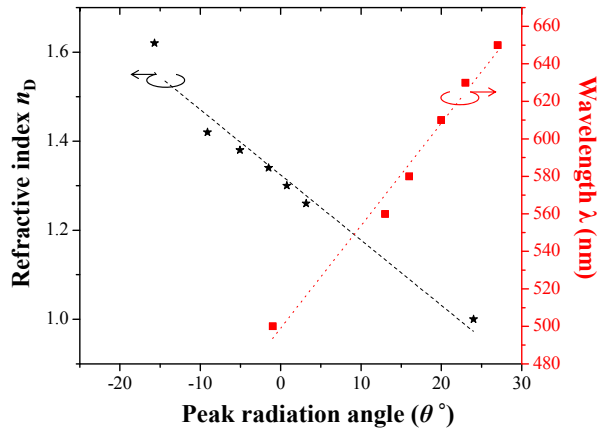


Fig. 5. Peak radiation angle as a function of wavelength (black) and the refractive index of surrounding medium (red). Each dashed line is a fitting curve for varying peak radiation angle.

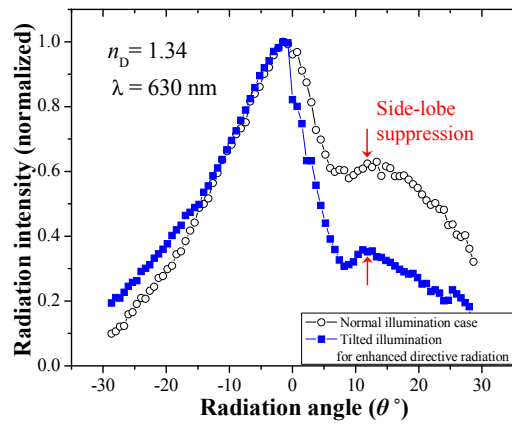


Fig. 6. Measured radiation patterns of the configuration shown in Fig. 1 for normal illumination (black curve, open circle) and tilted illumination (blue curve, filled box) for enhanced directive radiation. Index matching fluid with a refractive index of 1.34 was introduced and TM polarized light at 630 nm was used to excite the slit. Measured FWHM for normal incidence was 36.0°; whereas the case for tilted illumination was 19.1°.

As discussed above, it is important to note that the proposed geometry offers comparable sensitivity to conventional SPR based devices. For instance, the proposed configuration shows an angular sensitivity satisfying the relation  $\delta\theta_{DR} \approx -\delta\epsilon \cdot \lambda_0 / 2p$  upon the presence of small dielectric perturbations in the surrounding medium ( $\epsilon_D = 1 + \delta\epsilon$ ) if  $|\text{Re}(\epsilon_M)| \gg 1$  and  $|\delta\epsilon| \ll 1$  are assumed. Such sensitivity is comparable to that of conventional Kretschmann configuration [28], so we may find potential sensing applications based on dielectric perturbations.

## 5. Conclusion

In summary, we have experimentally demonstrated that the emission from a slit in a plasmonic screen may be directed in a specific direction of choice by coupling it with a compact grating system patterned on one side of the slit in the plasmonic surface. The radiation can be tuned to a large degree by varying the wavelength of operation and/or the index matching fluid surrounding the grating. Potential applications of this effect may be envisioned in tunable nano-optical devices and optical wireless links tunable in real-time. In addition, the sensitivity to such tuning mechanisms may be utilized for chemical and biomedical applications for which the spectral signature of samples could be identified.

## Acknowledgment

This research was performed in the Department of Biomedical Engineering, Microelectronics Research Center (MRC), and Center for Nano and Molecular Science (CNM) at the University of Texas at Austin. We gratefully acknowledge the financial support from NSF CAREER Award Grants (No. 0953311, PI: Alù, and No. 0846313, PI: Zhang) and the DARPA Young Faculty Award (N66001-10-1-4049, PI: Zhang).